JOC Article

# Photophysics and Electrochemistry of Conjugated Oligothiophenes Prepared by Using Azomethine Connections

Marie Bourgeaux and W. G. Skene*

*Department of Chemistry, University of Montreal, Pavillon J.A. Bombardier, C.P. 6128, succ. Centre-ville, Montreal, QC, H3C 3J7, Canada*

*w.skene@umontreal.ca*

*Received July 20, 2007*

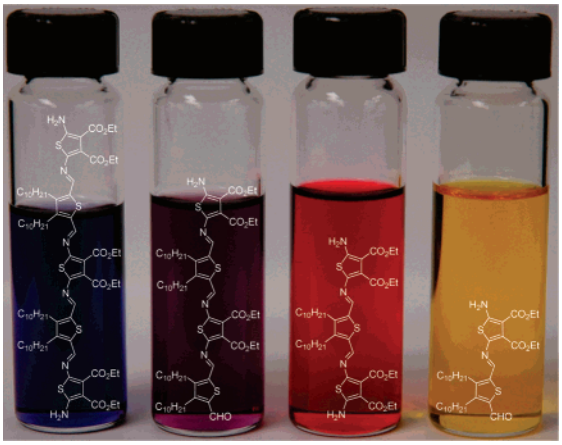

Novel conjugated azomethines consisting of 1 to 5 thiophenes and up to 4 azomethine bonds prepared from a stable diaminothiophene are presented. The effect of the number of thiophene and azomethines bonds on the photophysics and electrochemistry was examined. A high degree of conjugation was confirmed by bathochromic shifts upward of 120 and 210 nm for the absorbance and fluorescence, respectively, relative to the diaminothiophene precursor. Acid doping with methanesulfonic acid resulted in further bathochromic shifts along with lowering of the HOMO-LUMO energy gaps to 1.3 eV. Moreover, the compounds are extremely stable as evidenced by the absence of decomposition products under acid conditions. The resulting heteroatomic covalent bonds are furthermore reductively and hydrolytically resistant. Increasing the degree of conjugation shifts the nonradiative mode of singlet excited state energy dissipation from internal conversion (IC) to intersystem crossing (ISC). The resulting triplet manifold produced by ISC was efficiently deactivated by intramolecular self-quenching from the azomethine bond leading to a nonemissive triplet. Cyclic voltammetry revealed unprecedented reversible radical cation formation of the azomethines. Both one-electron oxidations and reductions were found by electrochemical measurements demonstrating the azomethines' capacity to be mutually p- and n-doped. One of the azomethines exhibited reversible electrochromic behavior with the electrochemically generated radical cation absorbing in the NIR at 1630 and 792 nm. X-ray crystallography confirmed the thermodynamically stable *E* isomer was formed uniquely and that the thiophenes are coplanar adopting an antiparallel arrangement.

## Introduction

Azomethines (−N═C−) are ideal alternatives to current coupling methods for the preparation of conjugated compounds. This is in part due to their properties that are isoelectronic to their carbon analogues.[1,2] They are advantageous to use as conjugated materials because of their ease of synthesis involving

* Address correspondence to this author. Fax: (514) 340-5290. Phone: (514) 340-5174.

(1) Wang, C.; Shieh, S.; LeGoff, E.; Kanatzidis, M. G. *Macromolecules* **1996**, *29*, 3147−3156.

(2) Yang, C.-J.; Jenekhe, S. A. *Chem. Mater.* **1991**, *3*, 878−887.

10.1021/jo701515j CCC: $37.00 
Published on Web 10/23/2007

the simple evaporation of the water byproduct. At the same time, their reaction protocols do not require the use of stringent reaction conditions or metal catalysts. Residual metal contamination requiring extensive purification is problematic for conventional conjugated material synthesis resulting in inconsistent physical properties in the final product.[3−5] Conjugated azomethines obtained by condensing complementary aryl amines with aldehydes not only yield robust covalent linkages, but also exhibit good hydrolytic and reductive resistance.[6−8] Concentrated acids in moist organic solvents are typically required to hydrolyze the bond while standard reductants fail to reduce the linkage even when refluxing in the presence of DIBAL.[6−8] The strength of the conjugated bond relative to unconjugated azomethines is epitomized by the extreme conditions required to hydrolyze and reduce the bond.

Common applications of conventional conjugated materials include organic light emitting diodes,[9−11] field effect transducers,[12−21] solar cells,[22−25] and conducting materials.[26−28] Synthetically appealing azomethines are potentially useful for such functional devices, though previous conjugated azomethines have not satisfied the stringent performance demands required for commercial applications.[29,30] This has been due predominately to the insufficient number of available stable aryl diamino precursors that are limited to phenylene diamine and its derivatives. Such homoaryl precursors are problematic because they are oxidized undesirably under ambient conditions while their azomethine products exhibit poor solubility, undesired oxidative decomposition, irreversible radical cation formation, inadequate emissions, and meager electrical/conductive properties. The limited number of stable diamino monomer precursors has unfortunately hindered the development of functional materials incorporating azomethines. This limiting factor can be overcome by using diaminothiophene analogues because the spectroscopic and electrochemical properties of thiophenes are compatible with functional devices. Azomethines incorporating such heteroaryl units would therefore possess ideal properties making them suitable for such devices.[6,31−33] Unfortunately, the required 2,5-diaminothiophene precursor for conjugated azomethines preparation is highly reactive and it cannot be isolated because it spontaneously decomposes under ambient conditions.

We recently addressed the challenge of conjugated azomethines with limited properties by using the stable 3,4-diethyl ester 2,5-diaminothiophene (**1**) as an azomethine precursor.[34−37] This compound is extremely air stable and it does not decompose under normal atmospheric conditions contrary to its unsubstituted analogue. In addition, **1** can be prepared in large quantities from inexpensive reagents in a one-step reaction, with high purity and through a simple crystallization.[33,38] The mutual-assembled condensation of **1** with 2-thiophene aldehydes yields conjugated azomethines consisting uniquely of thiophenes. Such compounds have renewed the interest in azomethines because of their promising properties that are compatible with functional materials including their use as hole injection materials in organic light emitting diodes.[6,31,32,39] The benefits of such azomethines consisting entirely of thiophene units, rather than their homoaryl analogues, include tunable spectroscopic properties, reversible radical cation formation, reversible p- and n-doping, low band gaps, and chemical resistance toward hydrolysis and azomethine reduction. They can also undergo controlled anodic electrochemical polymerization via the preferred α−α homocoupling to afford thin films of highly conjugated polymers similar to conventional thiophenes.[34,40,41]

Despite their extensive use and their well-studied behavior of protecting functional groups in organic synthesis, the photophysics and electrochemistry of conjugated azomethines have not been thoroughly examined. Moreover, the irreversible radical cation of homoaryl azomethines precludes their use as advanced

(3) Lavastre, O.; llitchev, I. I.; Jegou, G.; Dixneuf, P. H. *J. Am. Chem. Soc.* **2002**, *124*, 5278−5279.
(4) Kraft, A.; Grimsdale, A. C.; Holmes, A. B. *Angew. Chem., Int. Ed.* **1998**, *37*, 402−428.
(5) Leclerc, M. *J. Polym. Sci. Part A*: *Polym. Chem.* **2001**, *17*, 2867−2873.
(6) Thomas, O.; Inganäs, O.; Andersson, M. R. *Macromolecules* **1998**, *31*, 2676−2678.
(7) Kucybala, Z.; Pyszka, I.; Marciniak, B.; Hug, G. L.; Paczkowski, J. *J. Chem. Soc., Perkin Trans 2* **1999**, 2147−2154.
(8) Skopalová, J.; Lemr, K.; Kotouèek, M.; Èáp, L.; Barták, P. *Fresenius' J. Anal. Chem.* **2001**, *370*, 963−969.
(9) Rupprecht, L. *Conductive Polymers and Plastics in Industrial Applications*; Society of Plastics Engineers/Plastics Design Library: Brookfield, CT, 1999.
(10) Brabec, C. J.; Sariciftci, N. S.; Hummelen, J. C. *Adv. Funct. Mater.* **2001**, *11*, 15−26.
(11) Veinot, J. G. C.; Marks, T. J. *Acc. Chem. Res.* **2005**, *38*, 632−643.
(12) Katz, H. E.; Dodabalapur, A.; Bao, Z. In *Handbook of Oligo- and Polythiophenes*; Fichou, D., Ed.; Wiley-VCH Verlag GmbH: Weinheim, Germany 1999; pp 459−489.
(13) Thiem, H.; Strohriegl, P.; Setayesh, S.; Leeuw, D. d. *Synth. Met.* **2006**, *156*, 582−589.
(14) Dell'Aquila, A.; Mastrorilli, P.; Nobile, C. F.; Torsi, G. R. G. P. S. L.; Tanese, M. C.; Acierno, D.; Amendola, E.; Morales, P. *J. Mater. Chem.* **2006**, *16*, 1183−1191.
(15) Kraft, A. *Chem. Phys. Chem.* **2001**, *2*, 163−165.
(16) Horowitz, G. *Adv. Mater.* **1998**, *10*, 365−377.
(17) Perepichka, I. F.; Perepichka, D. F.; Meng, H.; Wudl, F. *Adv. Mater.* **2005**, *17*, 2281−2305.
(18) Dini, D. *Chem. Mater.* **2005**, *17*, 1933−1945.
(19) Kelley, T. W.; Baude, P. F.; Gerlach, C.; Ender, D. E.; Muyres, D.; Haase, M. A.; Vogel, D. E.; Theiss, S. D. *Chem. Mater.* **2004**, *16*, 4413−4422.
(20) Chen, C.-T. *Chem. Mater.* **2004**, *16*, 4389−4400.
(21) Parthasarathy, G.; Liu, J.; Duggal, A. R. *Interface* **2003**, 42−47.
(22) Colladet, K.; Fourier, S.; Cleij, T. J.; Lutsen, L.; Gelan, J.; Vanderzande, D.; Nguyen, L. H.; Neugebauer, H.; Sariciftci, S.; Aguirre, A.; Janssen, G.; Goovaerts, E. *Macromolecules* **2007**, *40*, 65−72.
(23) Velusamy, M.; Thomas, K. R. J.; Lin, J. T.; Hsu, Y.-C.; Ho, K.-C. *Org. Lett.* **2005**, *7*, 1899−1902.
(24) Thomas, K. R. J.; Lin, J. T.; Hsu, Y.-C.; Ho, K.-C. *Chem. Commun.* **2005**, 4098−4100.
(25) Segura, J. L.; Martín, N.; Guldi, D. M. *Chem. Soc. Rev.* **2005**, *34*, 31−47.
(26) MacDiarmid, A. G. *Angew. Chem., Int. Ed.* **2001**, *40*, 2581−2590.
(27) Dimitrakopoulos, C. D.; Malenfant, P. R. L. *Adv. Mater.* **2002**, *14*, 99−117.
(28) Holliday, B. J.; Swager, T. M. *Chem. Commun.* **2005**, 23−36.
(29) Suematsu, K.; Nakamura, K.; Takeda, J. *Colloid. Polym. Sci.* **1983**, *261*, 493−501.
(30) Morgan, P. W.; Kwolek, S. L.; Pletcher, T. C. *Macromolecules* **1987**, *20*, 729−739.
(31) Tsai, F.-C.; Chang, C.-C.; Liu, C.-L.; Chen, W.-C.; Jenekhe, S. A. *Macromolecules* **2005**, *38*, 1958−1966.
(32) Kiriy, N.; Bocharova, V.; Kiriy, A.; Stamm, M.; Krebs, F. C.; Adler, H.-J. *Chem. Mater.* **2004**, *16*, 4765−4771.
(33) Skene, W. G. 2005, US 60/541259.
(34) Bourgeaux, M.; Perez Guarin, S. A.; Skene, W. G. *J. Mater. Chem.* **2007**, *17*, 972−979.
(35) Pérez Guarìn, S. A.; Bourgeaux, M.; Dufresne, S.; Skene, W. G. *J. Org. Chem.* **2007**, *72*, 2631−2643.
(36) Dufresne, S.; Bourgeaux, M.; Skene, W. G. *J. Mater. Chem.* **2007**, *17*, 1166−1177.
(37) Bourgeaux, M.; Skene, W. G. *Macromolecules* **2007**, *40*, 1792−1795.
(38) Bourgeaux, M.; Vomscheid, S.; Skene, W. G. *Synth. Commun.* **2007**, *37*, 3551−3558.
(39) Skene, W. G. 2005, WO 2005073265.
(40) Guarìn, S. A. P.; Skene, W. G. *Mater. Lett.* published online April 19, http://dx.doi.org/10.1016/j.matlet.2007.04.015.
(41) Dufresne, S.; Gaultois, M.; Skene, W. G. *Opt. Mater.* http://dx.doi.org/10.1016/j.optmat.2007.05.031.

**CHART 1. Oligothiophenoazomethines Examined**

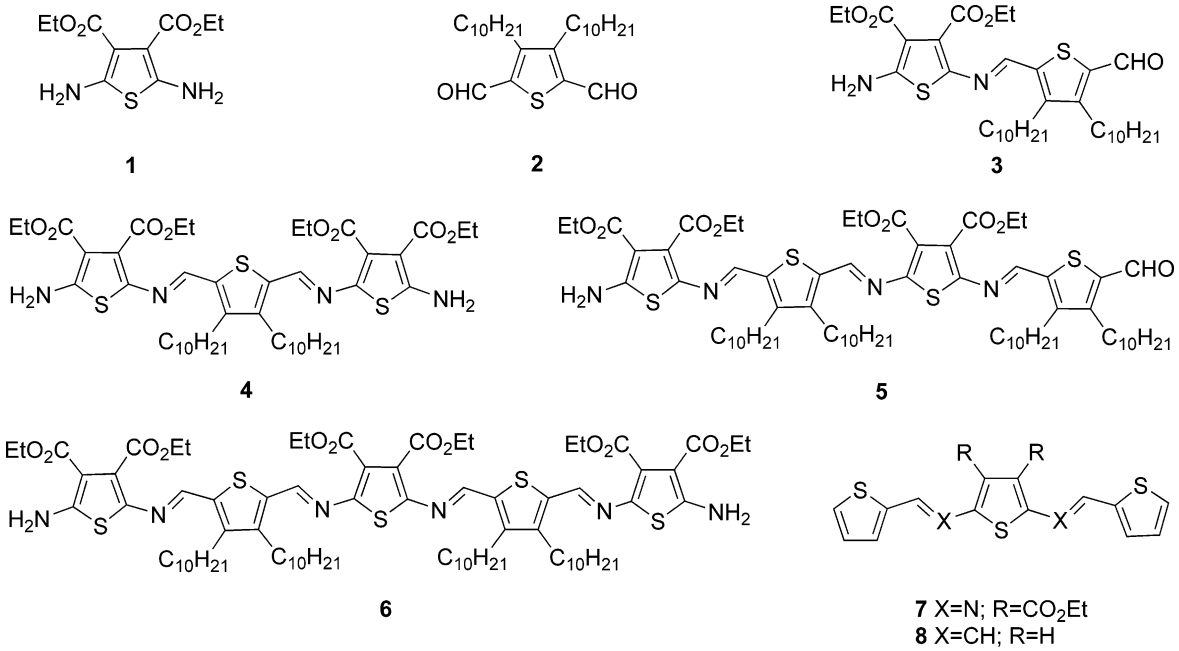


materials for electrochromic applications. Given the newness of thiophene containing azomethines and their potential uses for functional devices, structure−property relationship studies are crucial to ultimately assess their compatibility for such devices. Our recent novel conjugated azomethines[34−37,42,43] and the limited number of studies involving azomethines and their thiophene derivatives prompted us to investigate the effect of the number of thiophene units and the number of azomethine bonds in addition to the effect of the electronic donor and acceptors groups upon the photophysics and the electrochemistry of conjugated azomethines consisting entirely of thiophenes. This is of particular interest because it affords the means to better understand the main phenomena involved in the structure−property relationship while providing pivotal information for the future design and synthesis of thiopheno azomethines with desired characteristics. Information regarding the excited state including the singlet and triplet manifolds of azomethines and knowledge of their energy levels and redox potentials are essential for determining their suitability as advanced functional materials. We present such structure−property data of oligoazomethines consisting of 1 to 5 thiophenes including unprecedented electrochromism in addition to the crystallographic data.

## Results and Discussion

**Synthesis.** The synthesis of **1** is straightforward with inexpensive reagents and it can be isolated in high purity even on a g scale. Even though we previously reported the selective formation of **7** via judicious choice of solvent and reagent stoichiometry with 2-thiophene aldehyde and **1**, condensing stoichiometric amounts of **1** with its complementary dialdehyde **2** in acetone afforded the mixture of products reported in Chart 1. The overall yield of the condensation reaction was 84% while the predominate product isolated was **3** in approximately 54% yield followed by **4** (21%) and then **5** and **6** in equal amounts (7%). Interestingly, only the products reported in Chart 1 were isolated. No polymers were observed under the experimental conditions used even though they should have been formed. The electron withdrawing effect of the ester and the formed imine exert a combined effect to deactivate the terminal amine of **3**. This reduced reactivity not only explains the absence of polymers, but it is also responsible for the observed product ratios. The yield of **5** relative to **6** is much lower than expected because of the reduced reactivity of the terminal amines of **4** relative to **1**. Therefore, the condensation of **1** with **5** is preferred over the same reaction of **2** with either **4** or **5**. **1** therefore acts as a terminal capping group affording products with two terminal amines rather than products containing the complementary amine and aldehyde termini. The unusual product distribution notwithstanding, the preparation of a series of unprecedented oligomers with a varying number of thiophene units was possible from a one-pot synthesis. Moreover, the terminal aldehyde and amine groups lead to electronic *push*−*push* and *push*−*pull* conjugated compounds. This provides the means to examine the effect of the electronic groups on the physical properties of these novel compounds.

Although the compounds in Chart 1 are simple molecules resulting in straightforward $^{1}$H NMR spectra, the absence of distinctive aromatic protons renders absolute assignment difficult. The symmetry of **4** and **6** affords only one imine proton further making structural confirmation difficult by standard $^{1}$H NMR. The similar chemical shifts of the imine peaks and the absence of characteristic aryl protons for all the compounds caused further difficulties for the absolute characterization of the compounds, as seen in Figure 1. Furthermore, the peak at 7.52 ppm was cause for concern because it could not be assigned. Since amine protons readily exchange with deuterated solvents such as acetone, the unassigned peak was originally not thought to be the terminal amine. Confirmation of the desired products was done subsequently by using $^{15}$N−$^{1}$H 2D NMR, illustrated in Figure 2. This also allowed assigning the unidentified peak as the terminal amine. Despite this, absolute assign-

(42) Dufresne, S.; Bourgeaux, M.; Skene, W. G. *Acta Crystallogr., Sect. E*: *Struct. Rep. Online* **2006**, *E62*, o5602−o5604.
(43) Bourgeaux, M.; Vomsheid, S.; Skene, W. G. *Acta Crystallogr., Sect. E*: *Struct. Rep. Online* **2006**, *E62*, o5529−o5531.

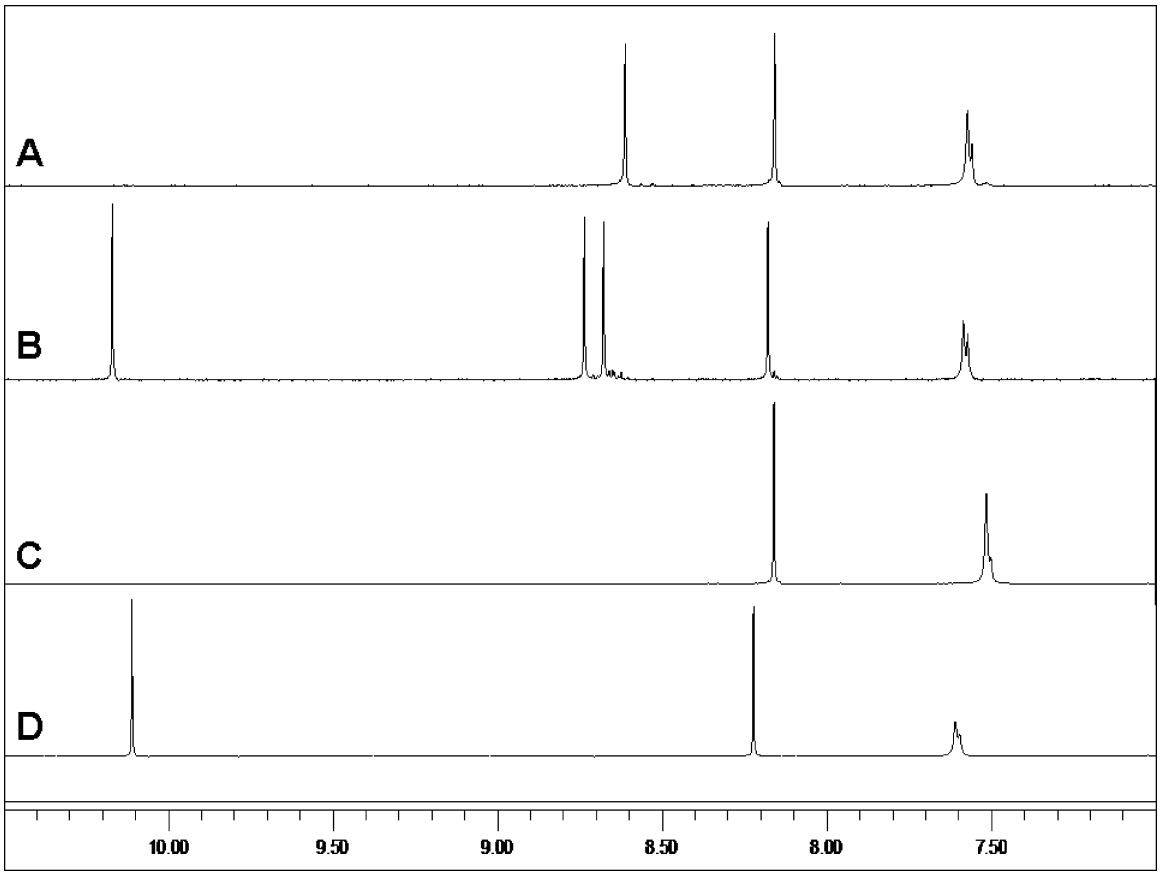


**FIGURE 1.** $^{1}H$ NMR spectra of thiophenoazomethines in deuterated acetone: (A) **6**, (B) **5**, (C) **4**, and (D) **3**.

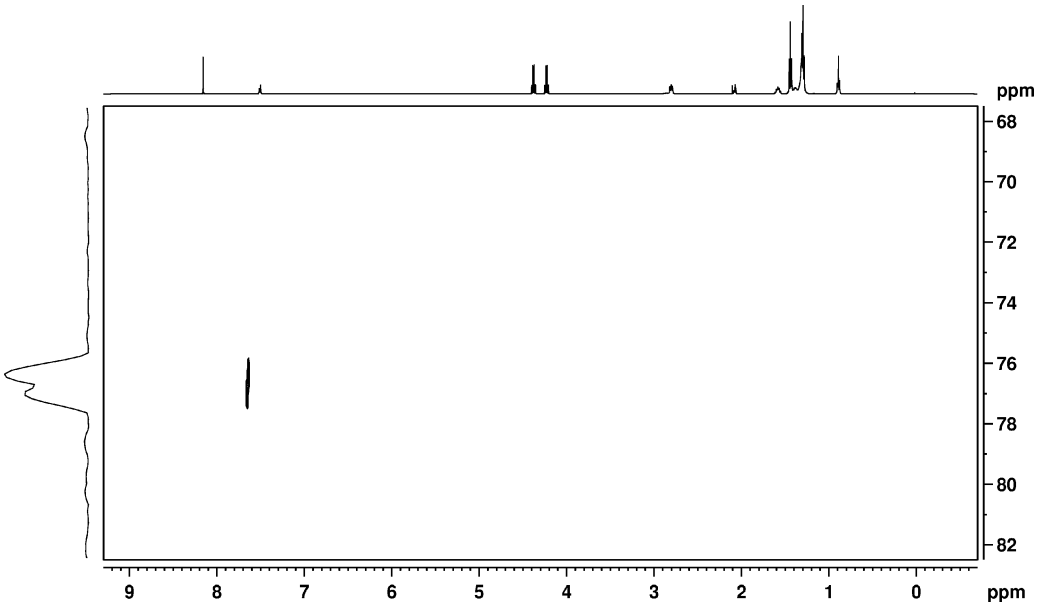


**FIGURE 2.** 2D NMR spectrum ($^{1}H$, $^{15}N$) of **4** correlating the protons and the amine nitrogen.

ment of the azomethine bond to either the *E* or *Z* geometric isomer was not possible by NMR and was only achievable by X-ray crystallography (vide infra).

**Spectroscopy/Photophysics.** Information pertaining to the ground and the excited states related to the HOMO and the LUMO energy levels, respectively, can be derived from the corresponding absorption and fluorescence spectra. The ground state absorption properties of the oligomers from Chart 1 are reported in Table 1. An average 50 nm bathochromic shift in the $\pi-\pi$ transition in the absorption spectra is observed in Figure 3 occurring with the addition of each thiophene. Not only does this trend confirm the increased degree of conjugation resulting from each thiophene addition, it also provides evidence that the compounds are linear and coplanar (vide infra). This is courtesy of the azomethine bond resulting in a high degree of delocalization. This is not surprising since previous crystal-

**TABLE 1. Spectroscopic Measurements of Various Oligothiopheno Azomethines Measured in Anhydrous and Deaerated Solvents**

| | dichloromethane | | | | | | thin films[a] | | 2-methyltetrahydrofuran | | | |
|---|---|---|---|---|---|---|---|---|---|---|---|---|
| compd | $\lambda_{abs}$[b] (nm) | $\lambda_{fl}$ (nm) | $\epsilon$ ($M^{-1}$ $cm^{-1}$) | $\Phi_{fl}$[c] ($10^{-3}$) | $\Delta E$[d] (eV) | $E_g$[b,e] (eV) | $\lambda_{abs}$ (nm) | $\lambda_{abs\ doped}$[b] (nm) | $\lambda_{abs}$ (nm) | $\Phi_{77K}$ | $\Phi_{77K}/\Phi_{fl}$ | $\Phi_{ISC}$[f] |
| **3** | 448 (583) | 552 | 30 500 | 0.9 | 2.5 | 2.4 (1.8) | 477 (513) | -[g] | 500 | 0.80 | 1000 | 0.20 |
| **4** | 504 (700) | 621 | 33 800 | 1.5 | 2.2 | 2.1 (1.5) | 514 | 683 | 518/560 | 0.31 | 180 | 0.69 |
| **5** | 549 (752) | 716 | 56 500 | 0.6 | 2.0 | 1.9 (1.4) | 560 | 731 | 580 | 0.09 | 60 | 0.91 |
| **6** | 576 (778) | 765 | 65 300 | 0.6 | 1.9 | 1.8 (1.3) | 602 | 742 | 615 | 0.002 | 40 | 0.99 |
| **7** | 440 (525) | 534 | 27 300 | 3 | 2.6 | 2.3 (2.0) | 440 | 512 | | 0.71 | 250 | 0.29 |
| **8**[h] | 351 | 422 | 24 200 | 50 | 3.1 | 3.2 | | | | | | |

[a] Refers to thin films deposited onto glass slides by spin coating from a dichloromethane stock solution. [b] Values in parentheses refer to properties measured after doping with methanesulfonic acid. [c] Fluoresence quantum yield at room temperature relative to fluorescein in alkaline ethanolic solution ($\Phi_{fl}$ = 0.92).[74] [d] HOMO-LUMO energy level difference measured from the intercept of the normalized absorption and emission spectra. [e] Spectroscopically determined HOMO-LUMO energy gap taken from the absorption onset. [f] $\Phi_{ISC} = 1 - \Phi_{fl}$(77K). [g] Polymerization occurred with acid doping. [h] From Becker et al.[46] and Wasserberg et al.[75] Reported values are measured in acetonitrile.

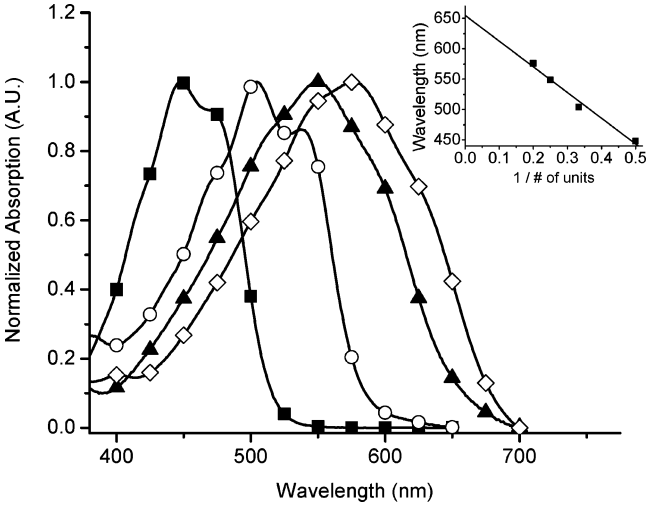


**FIGURE 3.** Normalized absorption spectra of **3** (■), **4** (○), **5** (▲), and **6** (◇) in dichloromethane. Inset: Absorption maximum as a function of thiophene units.

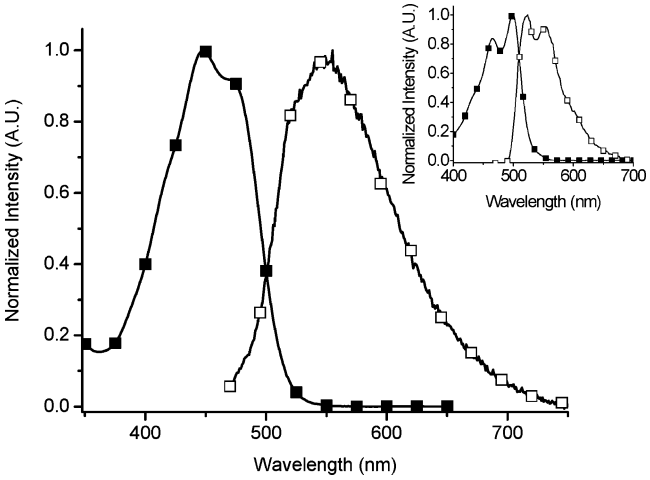


**FIGURE 4.** Normalized absorption (■) and emission (□) spectra of **3** in dichloromethane at room temperature. Inset: Normalized absorption (■) and emission (□) spectra of **3** in 2-methyltetrahydrofuran at 77 K.

lographic studies of thiophene derived azomethines have shown these compounds to be extremely linear and coplanar regardless of their substitution in the terminal positions.[34−36,42,44] The increased conjugation is further supported by the increase in the molar absorption coefficients observed with the addition of each thiophene and from the additional azomethine bond. The linear trend observed for the reciprocal number of thiophenes versus the absorption shift shown in the inset of Figure 3 supports the conjugated nature of the azomethine bond. Furthermore, the absorption of a polyazomethine consisting of alternating repeating thiophene units can be predicted by extrapolating the absorption data to infinity. The calculated value from the extrapolation method is 654 nm and is consistent with the experimental value of 663 nm for an analogous thiopheno polyazomethine confirming the extended $\pi$-conjugation of the compounds.[37]

The same bathochromic trend with the addition of each thiophene was also observed in the fluorescence spectra. The absorption and fluorescence data further provide information regarding the electronic effects of the terminal groups. This effect is obvious when comparing **7** with **4**. The 64 nm absorption difference between these two analogues is a result of the terminal electron donating amines. From the 87 nm fluorescence bathochromic shift calculated from Table 1, it is clear that the LUMO level is reduced to a greater extent than the HOMO level for **4** relative to **7**. This is not surprising since **4** possesses four electron withdrawing esters which are know to influence the LUMO level, while the donating amines perturb selectively the HOMO level. The terminal aldehyde also influences the spectroscopic properties. This electron withdrawing group causes a 48 and 72 nm bathochromic shift in the absorption and fluorescence spectra, respectively, relative to its aldehyde-free analogue.[36] The electron donating and withdrawing groups concomitant with the conjugation degree collectively contribute to influence the spectroscopic properties proving the means to tailor the spectroscopic properties for a given application.

The spectroscopic band gaps ($E_g$) and the absolute HOMO-LUMO ($\Delta$E) energy differences can be calculated from the spectroscopic data. The intercept of the normalized absorption and fluorescence spectra, illustrated in Figure 4, provides $\Delta E$, while $E_g$ is derived from the absorption onset. The latter method is valid because only a maximum difference of 25 nm was observed between the solution absorbance and that of thin films of variable thicknesses. Both methods confirm the same trend of decreasing energy difference resulting from an increasing degree of conjugation with each thiophene addition. The smallest energy difference was observed for **4**, while the subsequent addition of each thiophene resulted in a 0.2 eV lowering of the

(44) Skene, W. G.; Dufresne, S.; Trefz, T.; Simard, M. *Acta Crystallogr., Sect. E: Struct. Rep. Online* **2006**, *E62*, o2382−o2384.

HOMO-LUMO energy levels. Nonetheless, the lowest band gap of 1.8 eV was possible with **6** while that of its analogous polymer of $M_w = 15\,000$ g/mol is only 1.6 eV.[37]

The HOMO-LUMO energy gaps can be further decreased by protonating the amines with methane sulfonic acid resulting in a localized charge on the nitrogen. Even though such protonation decomposes other imines, no decomposition was observed either in solution or in thin films for the oligoazomethines studied. The absence of decomposition products further supports the robustness of the imine bond. The effect of the nitrogen protonation resulting in a dication is evident from the ca. 150 nm bathochromic shifts in the absorption relative to the corresponding unprotonated compounds. Protonation narrows the HOMO-LUMO energy gap by 0.6 eV leading to $E_g = 1.3$ eV for **6**. For comparison, the same narrow HOMO-LUMO energy gap was reported for a doped thiopheno azomethine polymer.[37] The similar low energy level difference for the oligomers and the polymer confirm the electronic groups can be exploited to tailor the spectroscopic properties similar to those achieved with high molecular weight polymers.

From Table 1, it is evident that the azomethine compounds fluoresce weakly as evidenced by their low fluorescence quantum yields ($\Phi_{fl}$). This is not surprising since thiophenes are generally understood to deactivate their singlet excited state preferentially by intersystem crossing (ISC) to the triplet manifold.[45−47] Conversely, azomethines were shown to dissipate their singlet excited state energy via internal conversion (IC).[34−36,48] Temperature-dependent studies were done to confirm the mode of nonemissive energy dissipation for **3**−**6**. 2-Methyltetrahydrofuran was selected as the solvent for the low-temperature measurements owing to its glass-forming capacity at 77 K concomitant with its capacity to dissolve the compounds of study. At this temperature, bond rotation is suppressed and singlet excited state deactivation by IC ($\Phi_{IC}$) can be confirmed by an increase in fluorescence intensity relative to room temperature measurements according to the following: $\Phi_{fl}$ (77K) − $\Phi_{fl}$ (rt) ≈ $\Phi_{IC}$. Similar to other thiopheno azomethines such as **7**, **3** dissipates its singlet excited state energy by IC evidenced by the 1000-fold fluorescence increase at 77 K relative to room temperature (Table 1). Even though this yields $\Phi_{fl} \approx 0.80$, a much higher value is expected given the error associated in comparing the extremely weak signal at room temperature relative to the intense signal observed at 77 K. This notwithstanding, a decreasing trend in the $\Phi_{77K}/\Phi_{rt}$ ratio was observed with each addition of a thiophene moiety. The change in the ratio indicates a trend of decreasing $\Phi_{IC}$ upon progressing from **3** to **6**. The extremely low $\Phi_{IC}$ value not only implies that the fluorescence at 77 K is dramatically reduced and is similar to that at room temperature, it also confirms a shift in the major mode of singlet excited state deactivation other than IC. A more efficient mode of energy dissipation therefore occurs with increasing the degree of conjugation. Given that we previously showed that azomethines are photostable,[34−37,48−50] the only available modes of singlet exited state energy dissipation are therefore accounted for by the following energy conversation equation: $\Phi_{fl} + \Phi_{ISC} + \Phi_{IC} \approx 1$. Since both $\Phi_{fl}$ and $\Phi_{IC}$ were measured, the conservation equation can be rewritten to calculate the amount of energy dissipated by ISC according to the following: $\Phi_{ISC} = 1 - \Phi_{IC}$ (77K). It is obvious from Table 1 that ISC to populate the triplet state becomes the preferred deactivation mode upon increasing the number of thiophenes and azomethine bonds. The increased degree of conjugation most likely lowers the singlet excited state favoring a symmetry-allowed transition from the singlet to the triplet and a subsequent $^1S \rightarrow S_0$ to $^1S \rightarrow {}^1T$ manifold shift.[51]

In addition to confirming the manifold shift for energy dissipation, qualitative information relating to structural changes is possible from the temperature-dependent fluorescence. As illustrated in the inset of Figure 4, both the absorption and the fluorescence spectra exhibit vibronic transitions at 77 K. The appearance of these transitions at the low temperature implies the HOMO-LUMO transition is well-defined and is consistent with a rigid and coplanar structure. The absorption is additionally bathochromically shifted by ca. 50 nm for all the compounds reported in Table 1. This confirms the oligomers are more conjugated at 77 K than at room temperature owing to the increased coplanarity resulting in the extended $\pi$-conjugation. This is confirmed by molecular orbital calculations of **4** by DFT-B3LYP, using the crystal structure geometry data for the single-point energy calculations. The distribution of the resulting HOMO and the LUMO levels (Figure 5) clearly shows that the HOMO is evenly distributed across the molecule while the LUMO is concentrated on the central thiophene and the azomethine bonds. This leads to an intramolecular charge transfer with significant distribution of the electronic density over the entire molecule. The large conjugated area provides an extended region across which the excited state can be efficiently dissipated. The net effect is an absence of any vibronic transitions in the observed absorption and the fluorescence spectra at room temperature owing to the mixing of the different vibrational levels.

Laser flash photolysis (LFP) was used to confirm the formation of the triplet state of **4**−**6** resulting from the manifold shift to ISC with increasing degree of conjugation. Direct excitation at 355 nm led to the transient absorption spectra shown in Figure 6. Even though the transient signal is weak compared to that of xanthone, the observed transients at 450 nm are indeed the triplets. This was confirmed by quenching the signal with triplet deactivators such as oxygen, methylnaphthalene, and 1,3-cycloxadiene in addition to the unimolecular decay kinetics observed in the absence of quenchers. Conversely, polarons or bipolarons would decay with biexponential kinetics because their disappearance would involve bimolecular recombination.

Given the strong ground state absorption of **4**−**6** in the visible region, a significant amount of ground state bleaching is noticeable in the transient absorption spectra. Quantitative kinetic information regarding the triplet quenching of these compounds was not possible owing to the pronounced bleaching seen as the negative signal in Figure 6. Alternatively, xanthone was used to probe the triplet deactivation capacity of **4**−**6** because it produces a strong triplet−triplet absorption signal that does not

(45) Seixas de Melo, J.; Elisei, F.; Gartner, C.; Aloisi, G. G.; Becker, R. S. *J. Phys. Chem. A* **2000**, *104*, 6907−6911.
(46) Seixas de Melo, J.; Fausto, E.; Becker, R. S. *J. Chem. Phys.* **2002**, *117*, 4428−4435.
(47) Seixas de Melo, J.; Silva, L. M.; Arnaut, L. G.; Becker, R. S. *J. Chem. Phys.* **1999**, *111*, 5427−5433.
(48) Pérez Guarìn, S. A.; Dufresne, S.; Tsang, D.; Sylla, A.; Skene, W. G. *J. Mater. Chem.* **2007**, *17*, 2801−2811.
(49) Pérez Guarìn, S. A.; Skene, W. G. *Mater. Lett.* published online Apr 19, http://dx.doi.org/10.1016/j.matlet.2007.04.015.
(50) Tsang, D.; Bourgeaux, M.; Skene, W. G. *J. Photochem. Photobiol. A* published online May 18, http://dx.doi.org/10.1016/j.jphotochem.2007.05.013.
(51) Turro, N. J. *Modern Molecular Photochemistry*; University Science Books: Sausalito, CA, 1991.

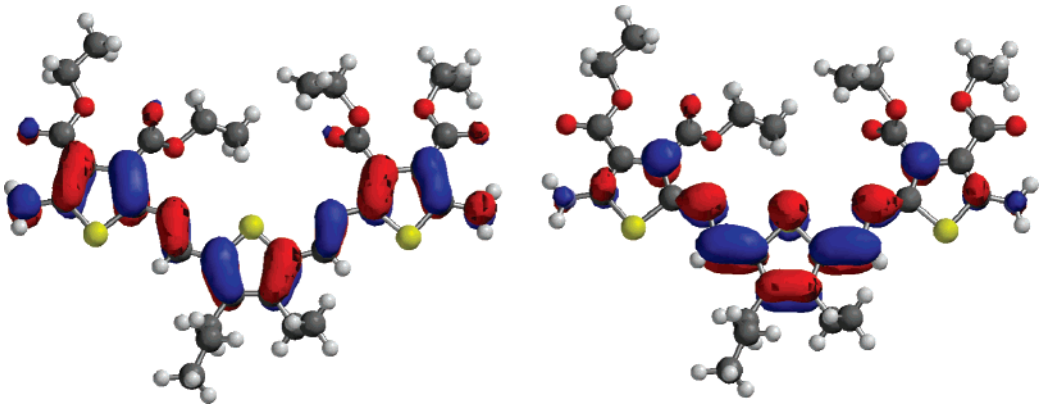

**FIGURE 5.** HOMO (left) and LUMO (right) surfaces of **4** calculated by DFT-B3LYP, using the 6-31g* basis set and taking the X-ray crystal data as the geometry for the single point energy calculations.

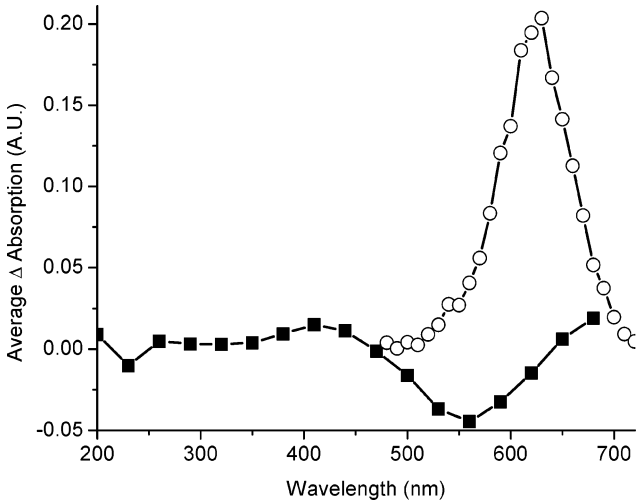


**FIGURE 6.** Transient absorption spectra of **6** (■) and xanthone (○) measured in deaerated dichloromethane at 27.8 and 1.4 $\mu$s, respectively, after the laser pulse at 355 nm.

overlap with the oligoazomethine triplets. Once again, accurate quenching results of triplet xanthone by **4**−**6** could not be obtained because of the strong absorption of the azomethines, which led to multiple transients. This problem notwithstanding, rate constants for quenching the triplet xanthone by the azomethines on the order of $10^{10}$ $M^{-1}$ $s^{-1}$ were observed. The diffusion-controlled quenching[52] rate constants not only confirm azomethine triplet quenching by Dexter energy transfer, they also suggest the triplet energies of **4**−**6** are lower than those of xanthone, whose $E_T$ = 255 kJ/mol.[51]

Even though the ground state bleaching of the azomethines prevents quantitative information regarding $\Phi_{ISC}$, additional qualitative information pertaining to the triplet state is possible by comparing the transient signal to that of xanthone. Given that the transient properties of xanthone are known ($\Phi_{ISC}$ = 1 and $\epsilon_{TT}$ = 28 000 $cm^{-1}$ $M^{-1}$),[53] comparing its signal to that of **4**−**6** obtained under the same conditions should provide a similarly intense signal according to eq 1. This is valid because two parameters contribute to the LFP signal: $\Phi_{ISC}$ and $\epsilon_{TT}$. Since the azomethines are highly conjugated, their $\epsilon_{TT}$ should be ≥12 000 $cm^{-1}$ $M^{-1}$. From the above energy conservation equation and from the estimated $\epsilon_{TT}$, the oligoazomethines should exhibit $\Phi_{ISC} \geq 0.2$. The azomethine LFP signal intensity should therefore be similar to that of xanthone despite the pronounced ground state bleaching. The unexpected weak signal can only arise from triplet deactivation occurring faster than the LFP's response time. Given that the shortest lifetime that can be resolved by the LFP system is 100 ns, the lack of any detectable triplet implies the intramolecular self-quenching of the triplet by the azomethine bond is extremely efficient. This rapid triplet self-quenching is consistent with our previous fluoreno azomethine studies.[48,54,55] This is supported by the absence of bimolecular rate constants that are association with radical ionic species concomitant with the absence of observed photodecomposition products after intense irradiation for 24 h at 350 nm. The LFP analyses provide indirect evidence that the triplet is produced and that it is rapidly self-quenched by the azomethine bond. Despite the rapid quenching, the spectroscopic data confirm a shift in the deactivation mode with increasing degree of conjugation such that **1**−**3** are deactivated by IC while the decreased singlet level of **4**−**6** favor ISC to form preferentially the triplet. The triply degenerate manifold is subsequently deactivated by nonradiative means.

$$\Phi_{azomethine} = \frac{\Delta Abs_{azomethine} \cdot \Phi_{xanthone} \cdot \epsilon_{xanthone}}{\Delta Abs_{xanthone} \cdot \epsilon_{azomethine}} \qquad (1)$$

**Electrochemistry.** The thiopheno azomethines undergo two stepwise one-electron oxidations corresponding to the radical cation followed by the dication. Even though the compounds studied from Chart 1 possess more than one thiophene, the specific thiophene that is oxidized cannot be unambiguously assigned. Regardless, the reversible oxidation process nonetheless occurred consistently at ca. 900 mV for all the compounds. Interestingly, formation of the azomethine radical cation is completely reversible, as represented in Figure 7. This is in stark contrast to previous examples of azomethines consisting of homologous aryl units that undergo irreversible oxidation. Not only are these earlier homoaryls irreversible oxidized,[56−59] they

(52) Montalti, M.; Credi, A.; Prodi, L.; Gandolfi, T. *Handbook of Photochemistry*, 3rd ed.; Marcel Dekker: New York, 2006.
(53) Carmichael, I.; Helman, W. P.; Hug, G. L. *J. Phys. Chem. Ref. Data* **1987**, *16*, 239−260.
(54) Skene, W. G.; Pérez Guarìn, S. A. *J. Fluores.* **2007**, *17*, 540−546.
(55) Tsanga, D.; Bourgeaux, M.; Skene, W. G. *J. Photochem. Photobiol. A* http://dx.doi.org/10.1016/j.photochem.2007.05.013.
(56) Diaz, F. R.; del Valle, M. A.; Brovelli, F.; Tagle, L. H.; Bernede, J. C. *J. Appl. Polym. Sci.* **2003**, *89*, 1614−1621.
(57) Zotti, G.; R.;andi, A.; Destri, S.; Porzio, W.; Schiavon, G. *Chem. Mater.* **2002**, *14*, 4550−4557.

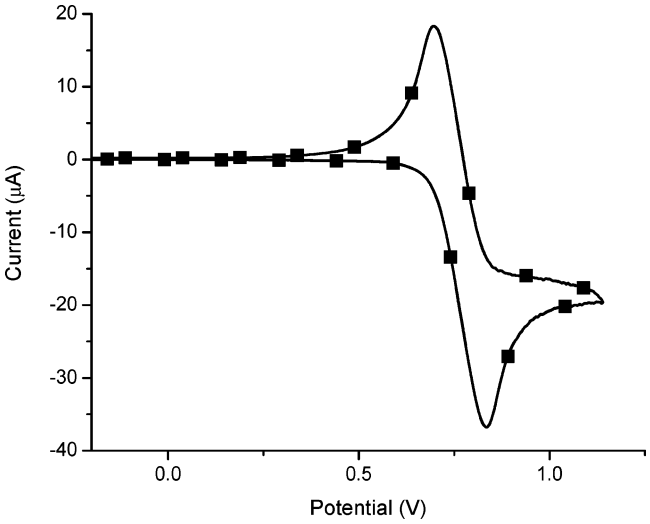


**FIGURE 7.** Cyclic voltammogram of **4** recorded in deaerated dichloromethane solution of 0.1 M of $TBAPF_6$, using Ag/AgCl as reference and Pt as working electrodes, respectively.

**TABLE 2. Electrochemical Data of Oligothiopheno Azomethines**

| | $E_{pa}^1$ (V) | $E_{pa}^2$ (V) | $E_{pc}$ (V) | HOMO (eV) | LUMO[a] (eV) | $E_g$ (eV) |
|---|---|---|---|---|---|---|
| **3** | 1.16 | 1.43 | −1.11 | −5.4 | −3.3 | 2.3 |
| **4** | 0.78 | | −0.91 | −5.1 | −3.5 | 1.7 |
| **5** | 0.90 | 1.16 | −0.83 | −5.3 | −3.6 | 1.7 |
| **6** | 0.86 | 1.22 | −0.81 | −5.2 | −3.6 | 1.7 |
| **7** | 1.00 | 1.30 | | −5.1 | −2.8a | 2.3 |
| **8**[b] | 0.88 | | | −5.2 | −2.6 | 2.6 |

[a] LUMO energy level calculated according to the following: LUMO = HOMO − $E_g$ (spectroscopic). [b] From Jérôme et al.[76,77]

also exhibited extremely high oxidation potentials. These undesired properties consequently limit their usefulness as functional materials.[6,56,59−64] The measured oxidation potentials ($E_{pa}$) are only slightly higher than their thiophene vinylene analogues of similar conjugation, such as **8**,[65,66] owing to the ester electron withdrawing group on the azomethine derivatives. However, the redox properties of the thiopheno azomethines can be tailored either by the use of electronic groups or by the degree of conjugation. For example, the two terminal amines collectively contribute to decrease the oxidation potential of **4** to 780 mV relative to its unsubstituted analogue (**7**), whose oxidation potential is 220 mV higher (Table 2). By comparison, the increased degree of conjugation attained by the addition of one thiophene is offset by the terminal electron withdrawing aldehyde of **5** resulting in a 120 mV increase in the $E_{pa}$ relative to **4**. Only a slight stabilization occurs with the addition of a thiophene as with **6** versus **5**. A significant reduction in $E_{pa}$ was expected with increasing degree of conjugation upon progressing from **3** to **6**. However, only an insignificant 40 mV reduction in the $E_{pa}$ was observed between **3** and **6**. The lack of pronounced $E_{pa}$ reduction is a result of the six-electron withdrawing groups that dominate the two terminal donating groups. The esters further counter affect any stabilization gained from the increased degree of conjugation. Despite this, the electrochemical data confirm the unprecedented reversible oxidation of the conjugated thiophenes. Furthermore, unmatched oxidation potentials below 800 mV are possible with the thiopheno azomethines.

Not only do **3**−**6** undergo an oxidation process demonstrating their p-doping type behavior, they also undergo a one-electron reduction. The reduction process observed for all the compounds is ascribed to a radical anion located on the thiophene moiety. Although the cathodic process demonstrates the capacity of these compounds to be n-doped, it does not correspond to the reduction of the imine bond since this is a two-electron process. Moreover, no chemical reduction was observed with standard reductants such as $NaBH_4$, $NaBH_3CN$, and DIBAL illustrating the robustness of the azomethine bond. The influence of the reduction potential by the electron withdrawing ester is obvious from the values reported in Table 2. The reduction potential was found to be inversely proportional to the number of ester groups confirming the stabilization effect of this electron withdrawing group on the $E_{pc}$.

The HOMO and LUMO energy levels were determined from the oxidation and reduction potentials, respectively. The ionization potential (IP) was calculated from the oxidation onset ($E_{onset}^{ox}$) according to IP = $E_{onset}^{ox}$(SEC) + 4.4, where $E_{onset}^{ox}$(SCE) is the oxidation potential onset in volts versus the SCE electrode. The LUMO energy level was similarly determined from the electron affinity (EA) from the reduction potential onset ($E_{onset}^{red}$) according to EA = $E_{onset}^{red}$(SEC) + 4.4. The difference between these two values provides the HOMO-LUMO energy difference ($E_g$). From the calculated values reported in Table 2, it can be concluded that the HOMO energy levels are approximately the same for all the compounds. Conversely, the LUMO is systematically lowered with each addition of **1** because each monomer adds more electron withdrawing esters, which influences the LUMO to a greater extent than the HOMO level. The electronic effect concomitant with the increased degree of conjugation moreover narrows the energy gap between the HOMO and the LUMO energy levels leading to $E_g$ values of 1.7 eV. The electrochemical values are corroborated by the spectroscopically measured values and also by the DFT calculation of 1.6 eV for **4**.

**Electrochromism.** The reversibility of the radical cation produced upon one-electron oxidation and its spectroscopy were further examined by spectroelectrochemistry. The change in absorption of **4** with various applied potentials is shown in Figure 8. Two new absorption peaks at 792 and 1630 nm occurred upon applying potentials greater than the $E_{pa}^1$ of **4**. Starting at 800 mV and increasing the potential in 50 mV increments resulted in absorption increases for the two peaks at 792 and 1630 nm concomitant with the decrease in the absorption intensity of neutral **4** at 504 nm. Since the potentials examined are similar to the first anodic process of **4** that is assigned to the radical cation formation, the hyperchromic spectral changes are assumed to be also from the radical cation intermediate. The 280 nm bathochromic absorption shift relative to the neutral

(58) Brovelli, F.; Rivas, B. L.; Bernede, J. C. *J. Chil. Chem. Soc.* **2005**, *50*, 597−602.
(59) Higuchi, M. Y.; Kimihisa. *Polym. Adv. Technol.* **2002**, *13*, 765−770.
(60) Yang, C.-J.; Jenekhe, S. A. *Macromolecules* **1995**, *28*, 1180−1196.
(61) Lund, H.; Hammerich, O. *Organic Electrochemistry*, 4th ed.; Marcel Dekker: New York, 2001.
(62) Caballero, A.; Tárraga, A.; Velasco, M. D.; Molina, P. *Dalton Trans.* **2006**, 1390−1398.
(63) Catanescu, O.; Grigoras, M.; Colotin, G.; Dobreanu, A.; Hurduc, N.; Simionescu, C. I. *Eur. Polym. J.* **2001**, *37*, 2213−2216.
(64) Grigoras, M. C.; Carmen, O.; Colotin, G. *Macromol. Chem. Phys.* **2001**, *202*, 2262−2266.
(65) Hansford, K. A.; Guarin, S. A. P.; Skene, W. G.; Lubell, W. D. *J. Org. Chem.* **2005**, *70*, 7996 -8000.
(66) Roncali, J. *Chem. Rev.* **1992**, *92*, 711−738.

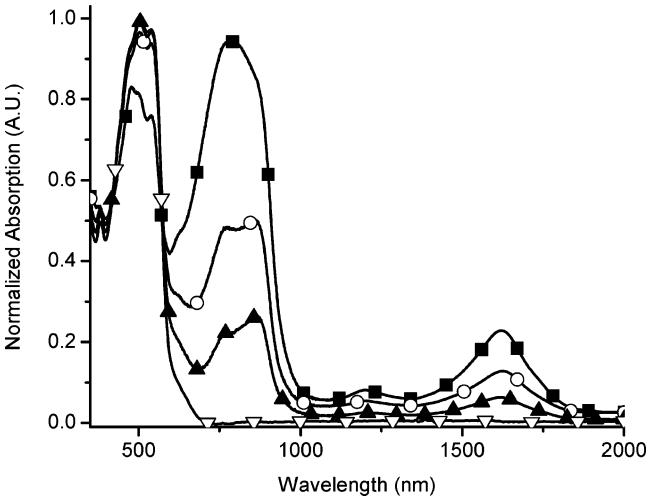


**FIGURE 8.** Voltage dependent spectroelectrochemical absorption spectra of **4** measured in dichloromethane at different potentials: 800 (▽), 850 (▲), 900 (○), and 950 mV (■).

compound implies the radical cation is highly conjugated and is 86 kJ/mol more stable than its neutral form. This is further supported by the spectroscopically derived HOMO-LUMO energy gap that is 0.5 eV lower than the neutral **4**.

To confirm the stability of the radical cation intermediate and the reversible behavior observed in Figure 7, the time-dependent spectroelectrochemistry was examined. Similar to the variable potential study, the absorption increase at 792 nm was proportional to the amount of time for which a given potential was applied. As seen in Figure 9, the intensity in the band at 792 nm increases with the simultaneous decrease in the absorption at 504 nm. The stability of the radical cation intermediate is evidenced by the absence of decomposition products that would otherwise result in significant changes in the absorption spectrum. Furthermore, the anodically induced spectral changes were persistent even after applying a potential for 12 min. The presence of a unique isobestic point at 571 nm provides additional confirmation that only two species are produced: **4** and $\mathbf{4}^{\bullet+}$. It additionally confirms that the two spectroscopically detected species are mutually derived. The absorption intensity at 504 nm was restored to its original intensity concomitant with the disappearance of the peak at 792 nm by applying a potential of −100 mV. Cycling between the potentials of 850 and −100 mV consistently gave the same absorption spectra. The absence of any degradation in the spectra and the consistent signal intensity concomitant with the single isobestic point further attest to the stability of the radical cation intermediate and the neutral **4**. The clean spectra provide further evidence for the azomethine bond robustness while the absence of spectral hysterisis confirms unprecedented reversible electrochromism.

**Crystal Structure.** Similar to their carbon analogues, two geometric azomethine isomers (*E* and *Z*) are possible. As seen in Figure 1, only one imine peak is visible in the 8−9 ppm region confirming the exclusive formation of one of the two possible isomers. Absolute assignment to either of the two azomethine isomers is not possible by $^1$H NMR; however, the most thermodynamically stable *E* isomer is assumed to be formed preferentially. Confirmation of the absolute geometry was possible from the crystal structure of **4** demonstrating the exclusive formation of the *E* isomer, shown in Figure 10.

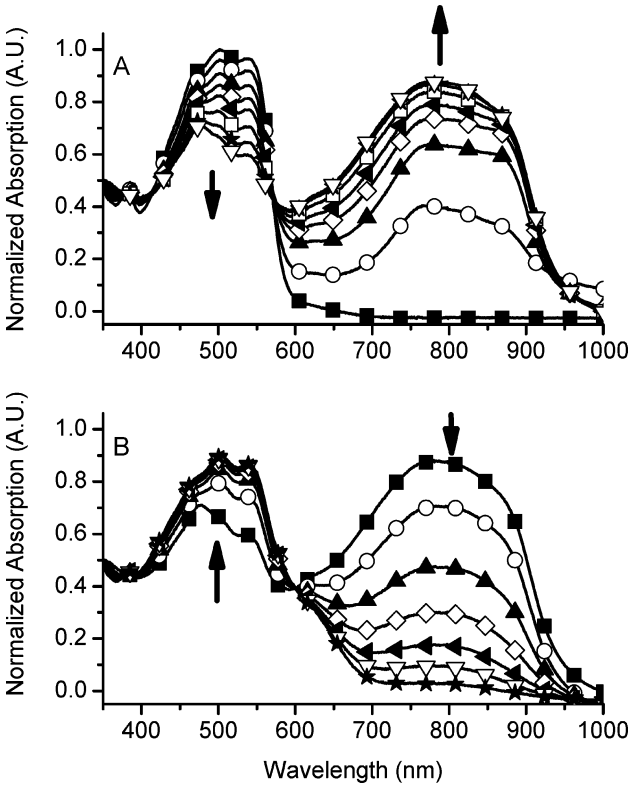


**FIGURE 9.** (A) Time dependent spectroelectrochemical absorption spectra of **4** measured in dichloromethane after applying a potential of +850 mV for 0 (■), 0.2 (○), 1.2 (▲), 2.2 (◇), 3.2 (rotated solid triangle), 5 (□), 8 (★), and 12 min (▽). (B) Time dependent spectroelectrochemical absorption spectra of **4** in dichloromethane obtained after applying a potential of −100 mV for 0 (■), 1.5 (○), 2.5 (▲), 3.5 (◇), 4.5 (rotated solid triangle), 5.5 (▽), and 7 min (★).

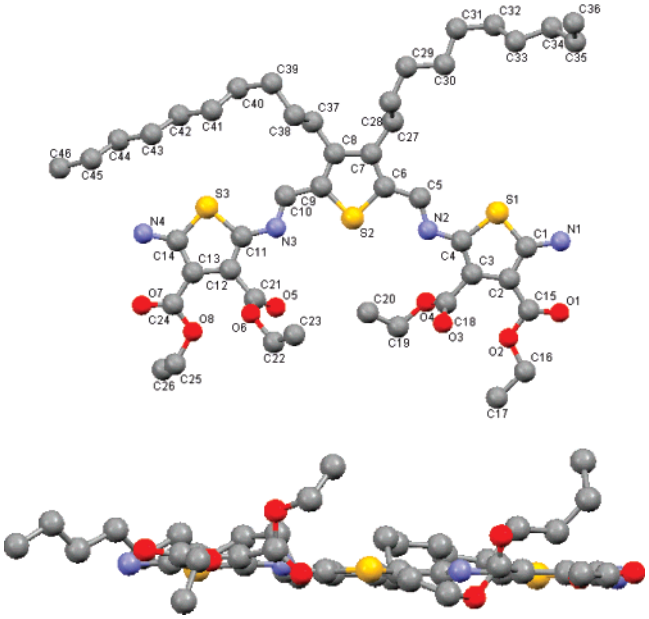

**FIGURE 10.** Crystal structure of **4** showing the numbering scheme (top) and seen along the axis parallel to the central thiophene ring (bottom).

The isolated crystal structure (Table 3) showed the heteroatomic rings are orientated in an antiparallel arrangement. This configuration is partly a result of intramolecular hydrogen

**TABLE 3. Details of Crystal Structure Determination of 4**

| formula | $C_{49}H_{76}N_4O_9S_3$ |
|---|---|
| $M_w$ (g/mol); $F(000)$ | 961.32; 1036 |
| crystal color and form | dark red |
| crystal size ($mm^3$) | 0.36 × 0.21 × 0.04 |
| $T$ (K); $d_{calc.}$ ($g/cm^3$) | 220 (2); 1.182 |
| crystal system | triclinic |
| space group | $P\bar{1}$ |
| unit cell | |
| $a$ (Å) | 11.8332(6) |
| $b$ (Å) | 13.9286(7) |
| $c$ (Å) | 17.0327(6) |
| α (deg) | 84.775(2) |
| $\beta$ (deg) | 83.451(2) |
| $\gamma$ (deg) | 76.160(2) |
| $V$ ($Å^3$); $Z$ | 2702.1(2); 2 |
| $\theta$ range (deg); completeness | 2.62−72.09; 0.951 |
| reflecns: collected/independent; $R_{int}$ | 29748/10113; 0.056 |
| $\mu$ ($mm^{-1}$); abs corr | 1.687; semiempirical |
| R1($F$); $wR(F^2)$ [$I > 2\sigma(I)$] | 0.1150; 0.3640 |
| R1($F$); $wR(F^2)$ (all data) | 0.1306; 0.3754 |
| GOF ($F^2$) | 1.134 |
| max residual $e^-$ density ($e^-\cdot Å^{-3}$) | 0.985 |

**TABLE 4. Selected Crystallographic Data of 4 and 7**

| | 4 | | 7[a] | |
|---|---|---|---|---|
| | side A | side B | side A | side B |
| plane angle[b] | 1.50° | 6.17° | 9.1° | 25.3° |
| −C═N− | 1.293 Å | 1.284 Å | 1.277 Å | 1.286 Å |
| ═N−Aryl− | 1.367 Å | 1.380 Å | 1.381 Å | 1.393 Å |
| ═CH−Aryl− | 1.435 Å | 1.443 Å | 1.443 Å | 1.435 Å |

[a] From Dufresne et al.[42] [b] Refers to the mean plane angle between the central thiophene and the terminal thiophene units.

bonding between the donor−acceptor pairs of the terminal sulfurs (S1 and S3) and the adjacent imine hydrogens (H5 and H10). The antiparallel orientation is similar to **7** in addition to other monoazomethines and bisazomethines.[34−36,42,44] As seen in Figure 10, the three thiophenes and the two imine bonds are coplanar. Only a 7° twist between the mean planes of the terminal thiophenes and the azomethine plane was observed (Table 4). The high degree of coplanarity is in contrast to those of homoaryl aromatic azomethines whose azomethine mean planes are normally twisted by 65° from the aryl units to which they are attached.[67−71] This arrangement places the imine hydrogen and that of the aryl ortho hydrogen in an energetically favored position as to avoid steric hindrance between the two hydrogens.[67,68] The deviation from coplanarity for such compounds limits their degree of conjugation.[72,73] The high degree of coplanarity of the aryl units and the azomethine bonds found

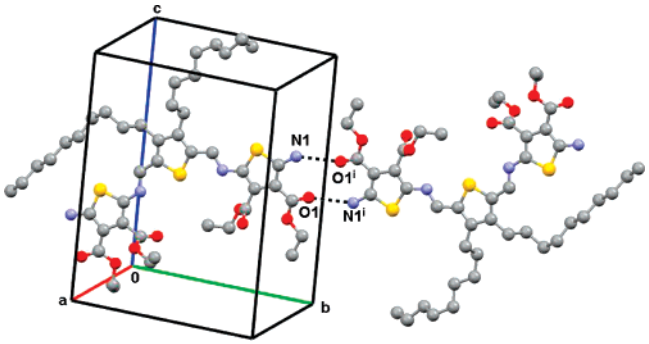


**FIGURE 11.** Supramolecular dimer representation of **4** showing the hydrogen bonds between the hydrogen donor terminal amine and the acceptor ester. The cell axes are shown for clarity [symmetry codes: (i) $-x, -y + 2, -z + 1$ and (ii) $x, y - 1, z$].

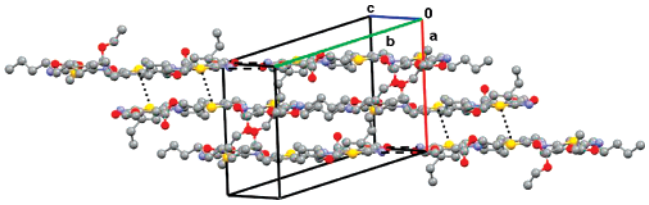


**FIGURE 12.** Crystal packing of **4** showing $\pi$-stacking (dotted line) and hydrogen bonds (dashed line) between different molecules in the unit cell. The cell axes are shown for clarity.

in the crystallographic data is responsible for the high degree of conjugation leading to reduced HOMO-LUMO energy gaps that also corroborate the spectroscopic results.

In addition to the weak S−H interaction, an additional intramolecular bond between a conventional donor−acceptor pair involving the terminal nitrogen and the ketone oxygen linking N1−O1 and N4−O7 was found. The strong nitrogen donor further forms an intermolecular hydrogen bond with the ketone from a different molecule of **4**. Two such interactions were observed involving the N1−O1$^{i}$ and N4−O3$^{iii}$ donor−acceptor pairs leading to a supramolecular dimer in which the two different molecules are coplanar as depicted in Figure 11. The two different molecules of **4**, participating in the dimer, adopt an antiparallel arrangement, and are separated by 2.984 (6) Å. $\pi$-stacking between different thiophenes in parallel planes also occurs providing a closed packing arrangement. Two such interactions take place per molecule between two parallel molecules that are separated by 3.554 (25) Å. The central and terminal thiophenes of one molecule $\pi$-stack with the terminal and central thiophenes of another molecule of **4**, respectively. This contributes to the ordered alternating brick-like crystal structure represented in Figure 12. This arrangement is further enhanced by $\pi-\pi$ interactions and the dimer hydrogen bonds leading to the ordered crystal structure.

## Conclusion

The first examples of azomethines consisting uniquely of thiophene units using a stable diaminothiophene ranging from 1 to 5 thiophenes were presented. The systematic study examining the effect of the number of azomethine bonds and thiophenes concomitant with the terminal electronic groups upon

(67) Skene, W. G.; Dufresne, S. *Org. Lett.* **2004**, *6*, 2949−2952.
(68) Skene, W. G.; Dufresne, S. *Acta Crystallogr., Sect. E*: *Struct. Rep. Online* **2006**, *E62*, o1116−o1117.
(69) Kuder, J. E. G.; Harry W.; Wychick, Darlene *J. Org. Chem.* **1975**, *40*, 875−879.
(70) Manecke, G.; Wille, W. E.; Kossmehl, G. *Makromol. Chem.* **1972**, *160*, 111−126.
(71) Bürgi, H. B.; Dunitz, J. D. *Chem. Commun.* **1969**, 472−473.
(72) Wan, C.-W.; Burghart, A.; Chen, J.; Bergström, F.; Johansson, L. B.-Å.; Wolford, M. F.; Kim, T. G.; Topp, M. R.; Hochstrasser, R. M.; Burgess, K. *Chem. Eur. J.* **2003**, *9*, 4430−4441.
(73) Jiao, G.-S.; Thoresen, L. H.; Burgess, K. *J. Am. Chem. Soc.* **2003**, *125*, 14668−14669.
(74) Murov, S. L.; Carmichael, I.; Hug, G. L. *Handbook of Photochemistry*, 2nd ed.; Marcel Dekker, Inc.: New York, 1993.
(75) Wasserberg, D.; Marsal, P.; Meskers, S. C. J.; Janssen, R. A. J.; Beljonne, D. *J. Phys. Chem. B* **2005**, *109*, 4410−4415.
(76) Jérôme, C.; Maertens, C.; Mertens, M.; Jérôme, R.; Quattrocchi, C.; Lazzaroni, R.; Brédas, J. L. *Synth. Met.* **1996**, *83*, 103−109.
(77) Jérôme, C.; Maertens, C.; Mertens, M.; Jérôme, R.; Quattrocchi, C.; Lazzaroni, R.; Brédas, J. L. *Synth. Met.* **1997**, *84*, 163−164.

the spectroscopic and electrochemical properties was possible. Each azomethine bond increased the degree of conjugation resulting in significant bathochromic shifts for both the absorption and fluorescence spectra. A shift in the deactivation manifold from IC to ISC occurred upon increasing the degree of conjugation while the triplet manifold was deactivated nonradiatively by intramolecular self-quenching. Even though high degrees of conjugation were found, that would otherwise decrease the oxidation potential significantly, the electron withdrawing esters offset this benefit resulting in oxidation potentials around 800 mV vs SCE. Despite the moderate oxidation potentials, unprecedented reversible radical cation formation was found in addition to low reduction potentials. The mutual oxidation and reduction confirm the conjugated thiophenes are both p- and n-dopable making these compounds suitable for advanced functional materials. In addition, the reversible color achieved upon oxidation makes the thiopheno azomethines ideal for uses in electrochromic applications. The advantage of the thiopheno azomethines is their simple synthesis such that the spectroscopic and electrochemical properties can be tailored by varying the number of thiophene units and the nature of the electronic groups substituted on the thiophenes.

## Experimental Section

**Synthetic Procedures: 2,5-Diaminothiophene-3,4-dicarboxylic Acid Diethyl Ester (1).** The same procedure as previously reported was used to synthesize the title compound.[38]

**3,4-Bis(decyl)thiophene-2,5-dicarbaldehyde (2).** 3,4-Dibromothiophene (4.89 g, 20 mmol) was dissolved into 100 mL of anhydrous THF, then [1,3-bis(diphenylphosphino)propane]nickel(II) chloride (200 mg, 0.4 mmol) was added. Three freeze−pump−thaw cycles were used to completely remove the residual oxygen. Decylmagnesium bromide (16.7 g, 67 mmol) was then added to the red solution, and the resulting brown solution was refluxed for 18 h. After cooling, the solution was passed through a plug of celite, then a plug of silica, and then it was finally washed with aqueous HCl (10% w/w). The organic layer was extracted with ethyl acetate and dried with $MgSO_4$, and the solvent was evaporated. The crude product was chromatographed on silica with 100% hexanes to afford a colorless oil (4.23 g, 58%). $^1$H NMR ($CDCl_3$) $\delta$ 6.89 (s, 2H), 2.50 (t, 4H, $J$ = 8.0 Hz), 1.61 (qt, 4H, $J$ = 8.0 Hz), 1.26 (br s, 28H), 0.88 (t, 6H, $J$ = 8.0 Hz). $^{13}$C NMR ($CDCl_3$) $\delta$ 144.1, 120.0, 32.9, 32.1, 30,8, 30.5, 30.2, 29.8, 29.6, 29.0, 22.9, 14.3.

To a solution of 3,4-bis(decyl)thiophene (1.70 g, 4.62 mmol) and freshly distilled TMEDA (2 mL, 12 mmol) in 30 mL of anhydrous hexanes under nitrogen was added dropwise to a solution of 2 M *n*-BuLi in hexanes (6 mL, 12 mmol). After refluxing for 1.5 h, THF (20 mL) was added and the solution was then cooled to −50 °C, to which DMF (2 mL, 27 mmol) was added dropwise. After 2.5 h at room temperature, the reaction mixture was hydrolyzed with water (60 mL) and the organic layer was extracted with ether. The combined organic layers were dried with $MgSO_4$ and then concentrated. The crude product was loaded onto a 40+M Biotage column and eluted with hexanes−ether up to 97%−3% (v/v) over 25 column volumes (CV) at 20 mL/min to give the product as a colorless oil (1.58 g, 81%). $^1$H NMR ($CDCl_3$) $\delta$ 10.11 (s, 2H), 2.90 (t, 4H, $J$ = 8.4 Hz), 1.59 (qt, 4H, $J$ = 8.4 Hz), 1.41 (qt, 4H, $J$ = 8.4 Hz), 1.26 (br s, 28H), 0.88 (t, 6H, $J$ = 8.40 Hz). $^{13}$C NMR ($CDCl_3$) $\delta$ 183.7, 152.1, 143.6, 32.6, 32.3, 30.0, 30.0, 29.9, 29.7, 27.0, 23.1, 14.5. HR-MS(+) calculated for $[C_{26}H_{44}O_2S + H]^+$ 421.31348, found 421.31405.

**Oligomers.** In 1 mL of acetone were dissolved **2** (200.0 mg, 0.47 mmol) and **1** (122.8 mg, 0.47 mmol) to which was then added 50 $\mu$L of a 1 M solution of TFA. The solution was heated to 40 °C for 24 h. The crude product was loaded onto a 24+M Biotage column and eluted first with hexanes/ether (90/10% v/v) up to 50/50% (v/v) over 20 CV at 20 mL/min to give a yellow solid (**3**; 156 mg, 48%) and a violet solid (**5**; 22 mg, 7%). The same column was then eluted with hexanes/THF (80/20% v/v) up to 65/35% (v/v) over 15 CV at 20 mL/min to give a red solid (**4**; 67 mg, 21%) and a blue solid (**6**; 18 mg, 6%). The overall reaction yield was 88%.

**2-Amino-5-[(3,4-bis(decyl)-5-formylthiophen-2-ylmethylene)-amino]thiophene-3,4-dicarboxylic acid diethyl ester (3).** $^1$H NMR (acetone-$d_6$) $\delta$ 10.11 (s, 1H), 8.22 (s, 1H), 7.61 (s, 1H), 4.35 (q, $J$ = 7.1 Hz, 2H), 4.21 (q, $J$ = 7.1 Hz, 2H), 2.99 (t, $J$ = 8.0 Hz, 2H), 2.87 (t, $J$ = 8.0 Hz, 2H), 1.62 (sext, $J$ = 8.0 Hz, 4H), 1.39−1.27 (m, 34H), 0.87 (t, $J$ = 7.5 Hz, 6H). $^{13}$C NMR (acetone-$d_6$) $\delta$ 183.2, 164.8, 164.2, 161.9, 152.5, 146.7, 144.8, 143.6, 139.8, 132.6, 132.5, 102.2, 61.2, 60.1, 32.5, 32.1, 32.0, 26.6, 26.4, 22.9, 14.3, 14.0, 13.9. Mp 92−94 °C. HR-MS(+) calculated for $[C_{36}H_{56}O_5N_2S_2 + H]^+$ 661.3703, found 661.3702.

**2-Amino-5-[(3,4-bis(decyl)-5-formylthiophen-2-ylmethylene)-amino]thiophene-3,4-dicarboxylic acid diethyl ester (4).** $^1$H NMR (acetone-$d_6$) $\delta$ 8.16 (s, 2H), 7.51 (d, $J$ = 5.5 Hz, 4H), 4.36 (q, $J$ = 7.1 Hz, 4H), 4.21 (q, $J$ = 7.1 Hz, 4H), 2.80 (t, $J$ = 8.0 Hz, 4H), 1.57 (sext, $J$ = 8.0 Hz, 1H), 1.48−1.19 (m, 40H), 0.87 (t, $J$ = 6.8 Hz, 6H). $^{13}$C NMR (acetone-$d_6$) $\delta$ 164.9, 164.3, 161.5, 147.0, 144.1, 140.4, 133.4, 131.0, 102.2, 61.1, 60.1, 32.2, 32.0, 26.7, 22.9, 14.4, 14.1, 13.9. Mp 129−133 °C. HR-MS(+) calculated for $[C_{46}H_{69}O_8N_4S_3 + H]^+$ 901.4272, found 901.4245.

**Diethyl 2-Amino-5-((*E*)-(3,4-didecyl-5-((*E*)-(5-((*E*)-(3,4-didecyl-5-formylthiophen-2-yl)methyleneamino)-3,4-bis(ethoxycarbonyl)thiophen-2-ylimino)methyl)thiophen-2-yl)methyleneamino)-thiophene-3,4-dicarboxylate (5).** $^1$H NMR (acetone-$d_6$) $\delta$ 10.17 (s, 1H), 8.74 (s, 1H), 8.68 (s, 1H), 8.18 (s, 1H), 7.59 (s, 2H), 4.45−4.28 (m, 6H), 4.22 (d, $J$ = 7.1 Hz, 2H), 3.08−2.87 (m, 8H), 1.74−1.54 (m, 8H), 1.53−1.14 (m, 68H), 0.93−0.79 (m, 12H). $^{13}$C NMR (acetone-$d_6$) $\delta$ 183.5, 164.8, 164.3, 163.0, 162.8, 161.9, 161.8, 152.4, 151.7, 151.0, 151.0, 150.7, 149.8, 148.2, 147.0, 143.6, 143.3, 141.7, 139.3, 133.2, 131.9, 129.6, 127.6, 102.3, 61.4, 61.3, 61.2, 60.1, 32.6, 32.2, 32.2, 32.1, 27.0, 26.7, 22.9, 14.5, 14.4, 14.3, 14.1, 13.9. Mp 128−130 °C. HR-MS(+) calculated for $[C_{72}H_{110}O_9N_4S_4 + H]^+$ 1303.7228, found 1303.7253.

**Tetraethyl 5,5′-(1*E*,1′*E*)-(5,5′-(1*E*,1′*E*)-(3,4-bis(ethoxycarbonyl)thiophene-2,5-diyl)bis(azan-1-yl-1-ylidene)bis(methan-1-yl-1-ylidene)bis(3,4-didecylthiophene-5,2-diyl))bis(methan-1-yl-1-ylidene)bis(azan-1-yl-1-ylidene)bis(2-aminothiophene-3,4-dicarboxylate) (6).** $^1$H NMR (acetone-$d_6$) $\delta$ 8.61 (s, 2H), 8.16 (s, 2H), 7.57 (d, $J$ = 5.46 Hz, 4H), 4.36 (sext, $J$ = 7.1 Hz, 8H), 4.22 (d, $J$ = 7.1 Hz, 4H), 2.85 (sext, $J$ = 8.7 Hz, 8H), 1.60 (m, 8H), 1.53−1.19 (m, 74H), 0.86 (q, $J$ = 6.8 Hz, 12H). $^{13}$C NMR (acetone-$d_6$) $\delta$ 164.8, 164.3, 163.0, 161.7, 151.0, 150.3, 149.7, 147.0, 143.8, 143.0, 139.4, 133.2, 131.8, 128.2, 102.3, 61.3, 61.2, 60.1, 32.2, 26.9, 26.7, 22.9, 14.4, 14.4, 14.1, 13.9. Mp 216−218 °C. HR-MS(+) calculated for $[C_{82}H_{122}O_{12}N_6S_5 + 2H]^+/2$ 772.3934, found 772.3917.

**Acknowledgment.** The authors acknowledge financial support from the Natural Sciences and Engineering Research Council Canada and the Centre for Self-Assembled Chemical Structures. Appreciation is extended to Dr. M. Simard and Mr. S. Dufresne for assistance with the crystal structure analysis and to Prof. D. Zargarian for helpful discussions. M.B. thanks the Université de Montréal for a graduate scholarship.

**Supporting Information Available:** $^1$H and $^{13}$C NMR spectra, absorption, fluorescence, and cyclic voltammograms, and the general characterization methods of compounds **3**−**6**. This material is available free of charge via the Internet at http://pubs.acs.org.

JO701515J